ACS OMEGA

Open Access

http://pubs.acs.org/journal/acsodf

Article

Physical–Chemical Assessment of Azo Dye Basic Violet I (BVI) Discoloration Using the Corona Plasma in Batch and Flow Systems

Aaron Gomez, María José Rodríguez Albarrán, Josefina Vergara Sanchez, Cesar Torres, Daniel Osorio, Horacio Martínez, Hugo Saldarriaga, and Pedro Guillermo Reyes*

Cite This: *ACS Omega* 2024, 9, 8037–8047

Read Online

ACCESS | Metrics & More | Article Recommendations

ABSTRACT: The decolorization of the Basic violet I (BVI) dye when interacted with a corona discharge is studied in the present work, taking in account two systems, batch and flux. The current and voltage were measured during the whole process in which a corona plasma was generated, with an applied power of 51.9 and 167.72 W where the transport gas was air. A batch reactor and a flow reactor were used, where 500 and 5000 mL of samples were treated, respectively. Optical emission spectra (OES) were measured where the oxidizing species ·OH were at wavelengths of 307.597 and 310.148 nm, associated with the $A^2\sum^+ - X^2\Pi$ transition. The absorption spectra for the batch system showed a discoloration of 85.7% in the first 10 min, while in the flow system, the absorption was 93.9% at the same time and 4.5% at the same time by conventional heating. Characteristics of the final sample included an acidic solution with an electrical conductivity of 449.20 ± 55.44 and 313.6 ± 39.58 μS/cm, a dissolved oxygen concentration of 7.74 ± 0.2 and 6.37 ± 0.23 mg/L, an absorbance of 0.04 ± 0.01 and 0.03 ± 0.01 au, with turbidity measuring 1.22 ± 1.59 and 10.34 ± 4.96 NTU, and an energy cost of 1.1×10^{-1} and 6.3×10^{-1} g/kWh in the batch and continuous flow systems, respectively. The interaction of the corona plasma with water promoted the production of reactive species, resulting in the discoloration of the Basic Violet I dye.

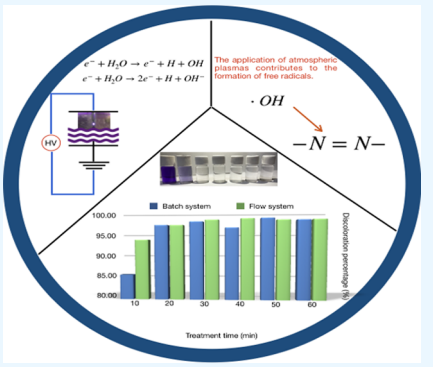

INTRODUCTION

In the literature, there are different works where the process of dye degradation is addressed using methods such as adsorption, biodegradation, ultrasonification,[1] photocatalysis,[2] and Fenton degradation.[3] However, these methods often require long treatment times, include the use of expensive compounds, and end up producing secondary contaminants that are more complex to degrade.[4]

According to the World Health Organization (WHO), the textile industry stands as one of the primary industrial polluters, accounting for 17 to 20% of global industrial wastewater. These wastewater streams contain toxic chemicals, reactive dyes, and alkaline and acidic compounds, rendering them harmful and hazardous to the environment and living organisms.[5] Particularly the Basic violet I dye is a chemical compound that can be harmful due to its toxicity. Some of the detrimental effects include water pollution, impacting aquatic life, and disrupting ecosystems. Moreover, if this dye contaminates the environment, it affects the food chain. Concerning soil alterations, it affects the soil's quality and fertility, reducing its ability for cultivation and plant life.

The degradation process of azo dyes dissolved in water has been studied using different methods, physical,[6] chemical,[7] and biological[8] or their combination.[9] This shows the high interest in the treatment of these residual waters since they are highly polluting, causing severe damages to the ecosystems in which they are discharged. Advanced oxidation processes (AOPs) are the most innovative technologies in wastewater treatments that can be used to degrade recalcitrant organics.[10]

There are different methods for removing dyes such as using the surface dielectric barrier discharge (SDBD) plasma method. In other studies, combinations of various processes are employed to enhance the degradation efficiency.[11] This includes advanced oxidation processes (AOPs) with non-thermal atmospheric pressure plasmas (NTAPPs). Among the chemical processes utilized is photocatalytic degradation (PD) applying nanophotocatalysts.[12]

An advanced method of oxidation that has taken relevance is the interaction of plasmas generated at atmospheric pressure using air as the carrier gas because it is found naturally in sufficient abundance to generate a plasma and does not require specific systems for its application. To generate a corona plasma, it is required to provide enough energy to ionize the

Received: October 18, 2023
Revised: January 6, 2024
Accepted: January 19, 2024
Published: February 8, 2024

https://doi.org/10.1021/acsomega.3c07559
ACS Omega 2024, 9, 8037–8047

carrier gas. The free electrons upon collision with the air remove electrons from the valence shells of the gas, thus generating the ionization process and becoming self-sustaining. Various chemical reactions occurred responsible for the formation of oxidizing species, which, given its characteristics, are capable of breaking double bonds responsible for the formation of azo dyes.[13] This process is essential to study under different fluid volume conditions to understand the degradation efficiency. The electric potential supplied contributes to the formation of free radicals, which can be formed under the following reactions: $e^- + H_2O \rightarrow e^- + H + OH$; $e^- + H_2O \rightarrow 2e^- + H + OH^-$; electronic impact, ionization and dissociation processes are present as the important atomic pathways.[14,15] Plasma production on the water surface is used to degrade organic contaminants in the water because not only hydroxyl radicals (·OH) but also atomic oxygen with a high oxidation potential can be produced.[44]

To achieve the formation of oxidant particles, different types of reactors have been developed with suitable configurations to generate plasmas at atmospheric pressure, which consider different basic variables: the energy required to achieve ionization of the system, the geometric configuration of the electrodes, as well as the type of material,[16] and the volume of the sample to be treated.[17] Methyl violet (MV) or pentamethylpararosaniline chloride ($C_{24}H_{28}N_3Cl$) is a common triphenylmethane dye, also called Methyl violet 2B or Basic violet I (C.I. 42535) (Figure 1).[18] This colorant is highly soluble in water and has great resistance to common treatments that include the use of photolysis from sunlight, common oxidizing agents, and aerobic attack.[19]

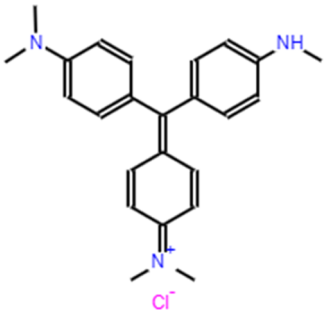

Figure 1. Molecular structure of Basic Violet I. This illustration has been based in part from the equilibrium and kinetic studies of methyl violet sorption by agricultural waste, Journal of Hazardous Materials (2008). 10.1016/j.jhazmat.2007.10.010. Copyright [2008 Journal of Hazardous Materials, Elsevier].

This dye is chiefly employed in the dyeing of cotton, silk, paper, bamboo, weed, straw, and leather, among others.[20]

The present work shows the results of the plasma treatment for the discoloration of the Basic violet I (BVI) dye at a 500 mL volume in a closed batch system and at 5000 mL in a flow-through system, at an initial concentration of 0.1 mM in both cases. The volumes show the potential for scale-up in the treatment of water with a textile dye. This method proves to be viable for applications in the discoloration of water containing textile dyes and potentially for the degradation of contaminants in the future.

EXPERIMENTAL SYSTEM

The experimental design aims to compare the treatment of water at different volumes with a textile dye through the interaction with a corona plasma, under the same physical and chemical conditions; for this, two systems were used, batch and flow. Treating a solution of distilled water with the textile dye (BVI), having a concentration of 0.1 mM, and adding $FeSO_4$ with a concentration of 0.1 mM from Meyer distribution, acting as the catalyst and supporting electrolyte due to the addition of Fe ions to the medium, significantly accelerates the degradation process because of the additional formation of OH, which generates H_2O_2 from Fenton's reaction.

The generation of the plasma used for the physical process of interaction with water was carried out in the Advanced Physics Laboratory, Autonomous University of the State of Mexico, where the plasma was characterized by optical emission spectroscopy (OES), in addition to the determination of the electrical variables. The experimental system used for the degradation is shown in Figure 2.[6] It consists of moving and fixed parts. A 500 mL beaker is closed with an airtight lid with ISO seals and three crosspieces, which contains the sample and is placed in the center of a rectangular chamber with no base and lid upper mobile, constructed with translucent acrylic. On one side of the chamber and the beaker, an optical fiber is placed, fixed with special mounting. The fiber is connected to an OCEAN OPTICS spectrometer HR4000CG-UV-NIR. In the mobile cover, there are three ports with ISO neoprene seals. Here, a condenser is connected whose shape is a tube of 3 cm in diameter and 10 cm in length to condense the formation of steam due to the heating of the sample, with

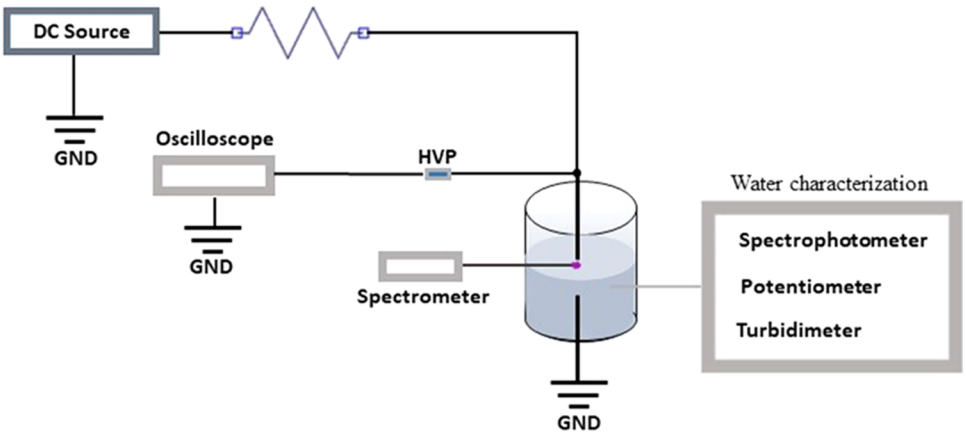

Figure 2. Batch system used for the degradation.

https://doi.org/10.1021/acsomega.3c07559
ACS Omega 2024, 9, 8037−8047

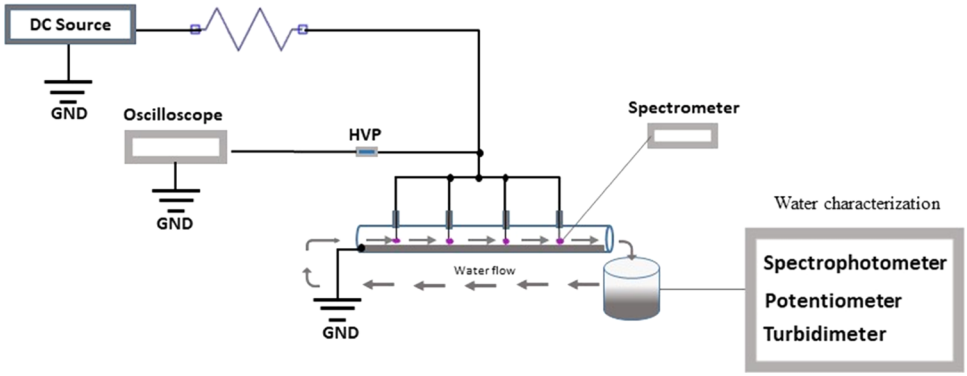

Figure 3. Flow system used for the degradation.

which a volume loss of less than 5% is achieved. A tungsten rod (100 mm long and 2 mm in diameter) is passed through the cover, serving as an electrode (anode) through which high voltage is applied to generate the plasma. This electrode is lowered with a ratchet and a guide support held by 4 guides and springs that stabilize the anode coupling to place it at the appropriate distance where the plasma zone occurs, which is 5 mm between the surface of the liquid and the tip of the electrode. The beaker has a tungsten electrode (cathode) of 30 mm in length and 2 mm in diameter at the bottom, always immersed in the solution. The discharge into the atmosphere−liquid interface is achieved by providing a flow of electrons through a high voltage power supply (130 mA, 1000 V), Keysight N8937A, which is monitored throughout the time of discharge with a Tektronix TDS 3014B, also simultaneously measuring the current with a multimeter BK Precision 5491B. Before and after each treatment, the measurements of pH and electrical conductivity were taken with a potentiometer HACH HQ40d.

The flow system (Figure 3) mainly consists of a glass tube being the tube through which the dye solution passes; this tube has an aluminum foil attached to the bottom, which is connected to the ground. The plasma is generated using a regulated high voltage source, which supplies current and voltage to 4 tungsten electrodes, equidistant, on the surface of the liquid, so that the interaction process has four points of contact with the sample in its trajectory inside the tube; the total volume treated is 5000 mL. The glass tube has a diameter of 23 mm and a large of 900 mm. Each one of the electrodes are mounted in an acrylic box for electrical insulation. Inside the boxes, there is a metallic mounting that keeps a tungsten rod acting like the electrode fixed; this configuration makes it possible to change the geometrical configuration for the electrodes. Inside the box, the electrodes are connected to high voltage, as shown in Figure 3. The system is configured for those four electrodes that could be placed in line for the treatment of the samples passing through the glass tube. Each of the electrodes can be raised and lowered, with the purpose of varying the separation distance between the electrode tip and the surface of the liquid sample; above each box is a handle through which it is possible to vary the height at which the electrode is positioned. Figure 3 shows the complete system; the four electrodes are fixed to an acrylic plate to align.

In the first instance, 5000 mL of water was prepared with the addition of 0.1 mM Basic Violet I dye and 1.0 mM $FeSO_4$ (iron sulfate); this quantity differs from the batch system to have the same treatment times since being of a greater volume, it takes more time, which acts as a catalyst and at the same time decreases the pH of the sample by increasing the conductivity. The sample prepared is supplied to the system by means of an electric submergible pump with a maximum capacity of 300 mL/min, limiting this flow using a mechanical valve until one flow of 100 mL/min with this flow set. A high voltage is applied to the electrodes, using a regulated power supply (Keysight N8937A), fixing values of 1000 V and 300 mA. The high voltage (anode) tip is connected to the electrodes with a ballast resistor of 1 kΩ, while the ground connection is made to the aluminum foil, acting as the cathode. One at a time, each electrode moves closer to the water surface until the point where there is an electric breakdown of air. This procedure is repeated with each of the following three electrodes, which allows to have four corona-type discharges generated at atmospheric pressure in the liquid−air interface.

The current and voltage parameters were monitored, in real time, by means of digital multimeters, BK PRECISION 5491B. Also, the optical emission spectrum was measured using an OCEAN OPTICS HR4000C−UV−vis spectrometer, with an optical resolution of 0.5 nm. Before and after each treatment, measurements of pH and electrical conductivity were taken with a potentiometer HACH HQ40d.

The determination of the number of treated samples was based on a study of the amount of wastewater generated by industries. According to official standards, a substantial statistical pool is necessary to ensure the efficacy of the method. For the physical and chemical characterization measurements of the water, a minimum of 400 mL of sample is required, with a total of 50 treated samples.

RESULTS AND DISCUSSION

Current−Voltage. The plasma generated in both systems for the interaction process is corona-type, and the average power required to form the plasma in the batch system is 51.9 W, while in the flow system, it is 167.7 W due to the fact there are 4 interaction points, where the current and voltage are the same in each interaction point, this being the minimum energy required for the discharge to be self-sustained. The variations in power observed for the batch system are due in part to volume loss, which changes the separation distance between the surface and electrodes and also to due to sample evaporation, which produces changes in the atmospheric density locally at the interaction points, while for the flow system, the most evident changes are due to volume loss by evaporation. The behavior of both curves is influenced by changes in electrical conductivity. When the discharge is

https://doi.org/10.1021/acsomega.3c07559
ACS Omega 2024, 9, 8037−8047

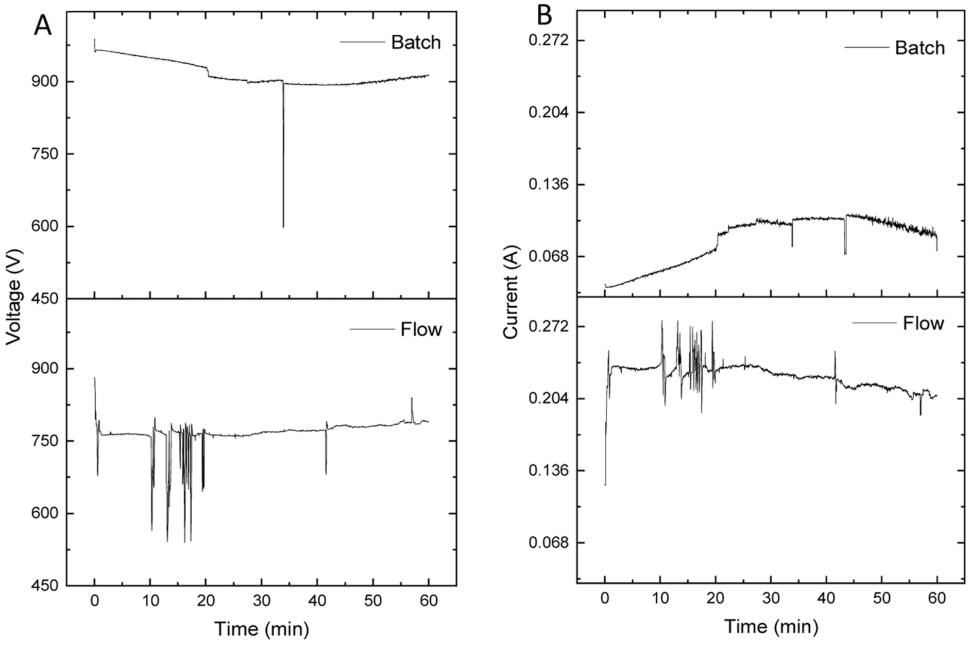

Figure 4. (A) Voltage for batch and flow systems. (B) Current for batch and flow systems.

generated in both systems, they remain self-sustained. The results obtained by monitoring the mentioned parameters during the whole treatment time indicate that in the batch system, a lower voltage is used (Figure 4A), between 900 and 960 V, noting that in the flow system, the voltage is maintained close to 771 and 788 V. This is due to a higher energy that the flow system requires to keep the four interactions points stable. The current (Figure 4B) required for the closed system is between 0.03 and 0.08 A, while for the flowing system, it is between 0.20 and 0.23 A.

Optical Emission Spectra (OES). For both cases, batch and flow systems, optical emission spectra were obtained and analyzed at all treatment times 10, 20, 30, 40, 50, and 60 min, as shown in Figure 5. The normalized comparison of the optical emission spectra is observed, as a function of the maximum peak.

For spectroscopic analysis and study of the evolution of the discharge with respect to time, spectra were taken for each treatment time for both systems, in which the same species are observed. The species present are ·OH, N_2, H_β, and H_α. ·OH wavelengths corresponding to the band in the range between 307.597 and 310.148 nm are associated with the transition $A^2\sum^+ - X^2\Pi$[21] since the plasma is generated at the liquid−air interface. N_2 species are expected to be present, observed at the wavelengths 315.03, 338.72, 358.2, 392.88, 399.09, 409.13, and 420.14 nm; these species correspond to the transition $C^3\Pi_u - B^3\Pi_g$.[22] Hydrogens H_β are also found at the wavelength 486.05 nm on the transition $n = 2$ *a* $n = 4$, in addition to H_α at the wavelength 656.48 nm at the levels $n = 2$ *a* $n = 3$.[23] Table 1 shows the species observed. In the first column, under experimental system, number 1 refers to the species observed in the batch system and number 2 refers to those observed in the flow experimental system.

As can be seen in Figure 5 and Table 1, the number of species identified by OES is diverse. Some of the reactions that occurred in the atmospheric plasma and were identified in OES are as follows[13]

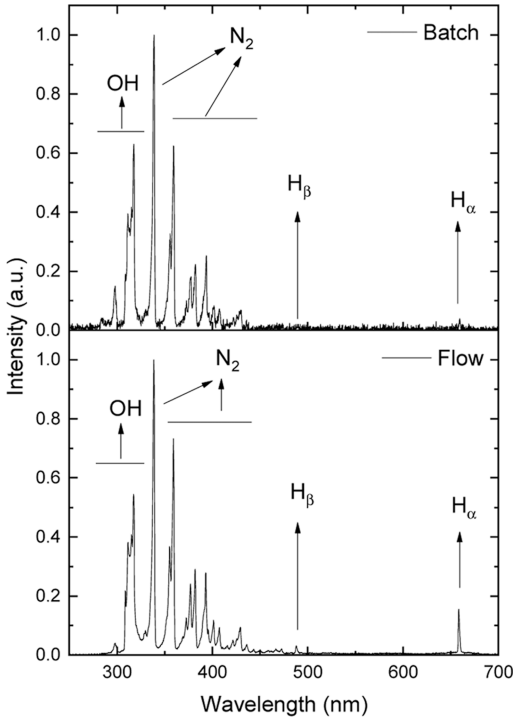

Figure 5. Comparison of optical emission spectra in batch and flow systems.

$$e^- + N_2 \rightarrow N_2^* + e^- \quad (1)$$

$$e^- + N_2 \rightarrow N + N + e^- \quad (2)$$

$$e^- + O_2 \rightarrow O + O + e^- \quad (3)$$

$$e^- + O_2 \rightarrow O_2^+ + 2e^- \quad (4)$$

$$e^- + O_2 + M \rightarrow O_2^- + M \quad (5)$$

where eq 1 expresses the excitation process and it justifies the identification of N_2 bands in the optical emission spectrum;

https://doi.org/10.1021/acsomega.3c07559
ACS Omega 2024, 9, 8037−8047

Table 1. Numbers 1 and 2 Refer to Experimental Systems (1: Batch System) and (2: Flow System)[a]

Experimental system	Intensity (a.u.)	Species	Experimental wavelength (nm)	Theoretical wavelength (nm)	Transition
1	0.045	·OH	307.59	307.8	$A^2 \sum^+ - X^2 \Pi$
2	0.023				
1	0.197	·OH	310.15	308.9	$A^2 \sum^+ - X^2 \Pi$
2	0.197				
1	0.416	N_2	315.03	315.93	$C^3 \Pi_u - B^3 \Pi_g$
2	0.408				
1	0.957	N_2	338.72	337.13	$C^3 \Pi_u - B^3 \Pi_g$
2	1				
1	0.426	N_2	358.2	357.69	$C^3 \Pi_u - B^3 \Pi_g$
2	0.491				
1	0.177	N_2	392.88	392.5	$C^3 \Pi_u - B^3 \Pi_g$
2	0.272				
1	0.033	N_2	399.09	399.84	$C^3 \Pi_u - B^3 \Pi_g$
2	0.059				
1	0.019	N_2	409.13	409.505	$C^3 \Pi_u - B^3 \Pi_g$
2	0.028				
1	0.025	N_2	420.14	420.007	$C^3 \Pi_u - B^3 \Pi_g$
2	0.034				
1	0.005	H_β	486.05	486.133	$n = 2$ *a* $n = 4$
2	0.018				
1	0.022	H_α	656.48	656.29	$n = 2$ *a* $n = 3$
2	0.010				

[a]The species were observed by optical emission spectroscopy. This table has been based in part from The Identification of Molecular Spectra, Chapman and Hall Ltd. 1976.

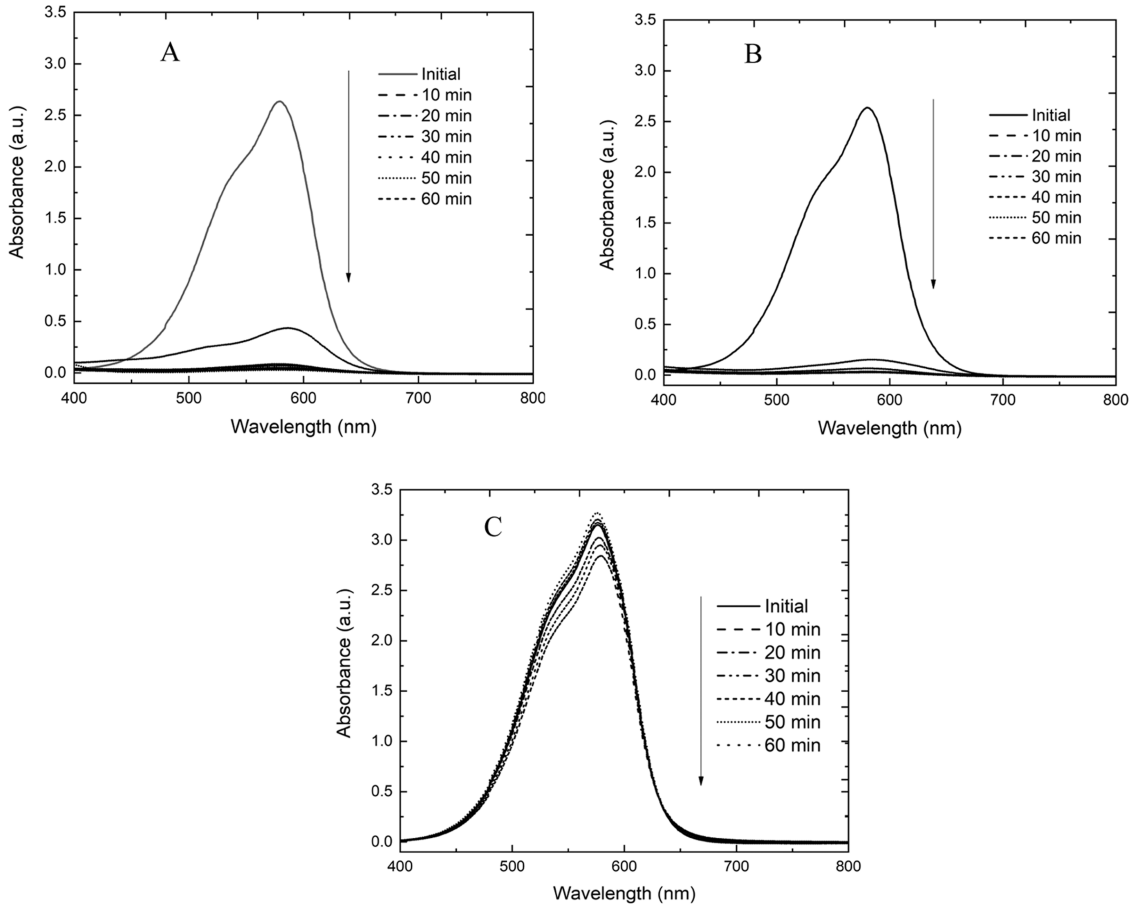

Figure 6. Absorption spectra in (A) the batch system, (B) the flow system, and (C) the hot plate.

eqs 2 and 3 show an example of the dissociation process; eq 3 shows the formation of oxygen by electron impact; eq 4 shows the ionization of oxygen molecules; and eq 5 expresses the electron capture, where M is the third collision partner, which

https://doi.org/10.1021/acsomega.3c07559
ACS Omega 2024, 9, 8037−8047

may be O_2 or N_2. All reactions were of high-energy electrons in the atmospheric plasma in air.

When atmospheric plasmas interact with water, a series of chemical and physical reactions can occur. Generally, plasmas can generate reactive species of oxygen and nitrogen, such as hydroxyl (·OH) radicals and nitrite ($\cdot NO_2$) or nitrate ($\cdot NO_3$) radicals. These radicals can interact with water components and lead to the formation of nitrates (NO_3^-) and nitrites (NO_2^-).

Absorption Spectra (AS). The discoloration process is mainly due to the interaction of the dye molecules with the · OH radicals formed within the liquid. These radicals, being highly oxidizing, break the nitrogen double bonds in the first instance, thus generating the discoloration effect of the sample.

Figure 6 shows the absorption spectra at the treatment times 0, 10, 20, 30, 40, 50, and 60 min with the plasma of the samples by the batch system (Figure 6A), the flow system (Figure 6B), and heating in a hot plate (Figure 6C). The theoretical maximum absorption wavelength is 584 nm, reported by the dye manufacturer. The uncertainty is determined by statistical analysis using the mean standard deviation of the average of the total of the measurements. It is observed that the absorbance, as shown in Figure 7, is reduced in a percentage of 85.7, 97.3, 98.1, 96.7, 98.9, and 98.5, respectively, in the batch system, while for the flow system, the percentage is 93.9, 97.3, 98.5, 98.8, 98.5, and 98.6. So, it is possible to say that at 20 min, the treatment is efficient for the degradation of the dye in both cases, observing that at 10 min of interaction, the treatment in the flow system is more efficient due to the 4 points of interaction during the process; however, at 60 min, the result is the same. By effect of the plasma interaction, the water temperature is elevated up to 90 °C at 60 min. It could be assumed that this change is not responsible for the breaking of the chromophore bonds. With the purpose of verifying this assertion, the sample was heated in a hot plate at the same time as the plasma interaction, resulting in minimal discoloration.

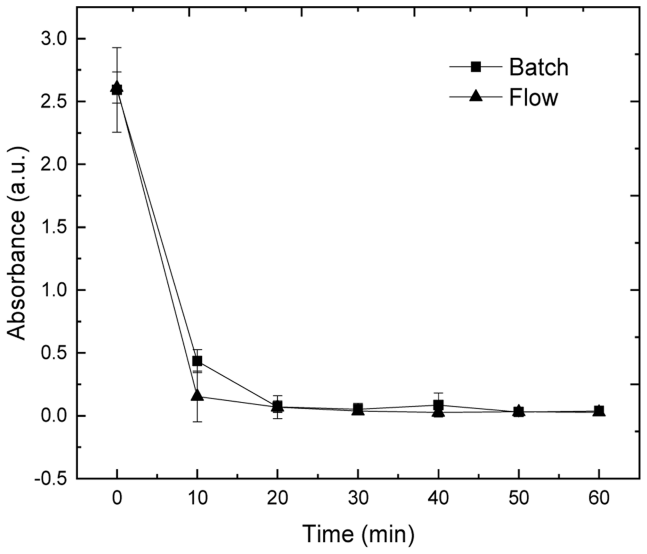

Figure 7. Discoloration percentage.

Figures 8 and 9 show the samples at the different interaction times, and the discoloration is evident, with a difference in the time of 10 min where the flow-through system is more efficient.

pH−Electrical Conductivity. Due to the production of hydrogen ions and the concentration that exists in the solution, it is determined whether a solution is acidic or alkaline. Specifically, the dye solution used, after 10 min of treatment, maintains an acidic pH. This is largely due to the added catalyst, in addition to the fact that in acid solutions, it facilitates the production of hydroxyl radicals. Also, a difference is observed with respect to the behavior in the different systems. In the batch system, the pH value decreases, while in the flow system, this value increases, thus inferring the behavior of electrical conductivity. As shown in Figure 10, in the batch system, the electrical conductivity value increases, and in the flow system, it decreases, this being corroborated with the results. This behavior is associated with the temperature of the solution and with the fact that closed and open systems cause a higher or lower interaction of hydrogen ions with the environment, as shown in Figure 11.

In both flow and batch systems, when the plasma interacts with the solution, some of the chemical variables of the solution change, for example, EC and pH, which are affected because the system is supplied with high-energy electrons due to the effect of plasma generation on the water surface, causing ionization, dissociation, and recombination processes with water molecules, generating ·OH and ·H radicals,[25,26] as described in the following reaction (eq 6):

$$H_2O + e^- \rightarrow \cdot OH + \cdot H + e^- \quad (6)$$

Figure 8. Time-dependent degradation in the batch system.

https://doi.org/10.1021/acsomega.3c07559
ACS Omega 2024, 9, 8037−8047

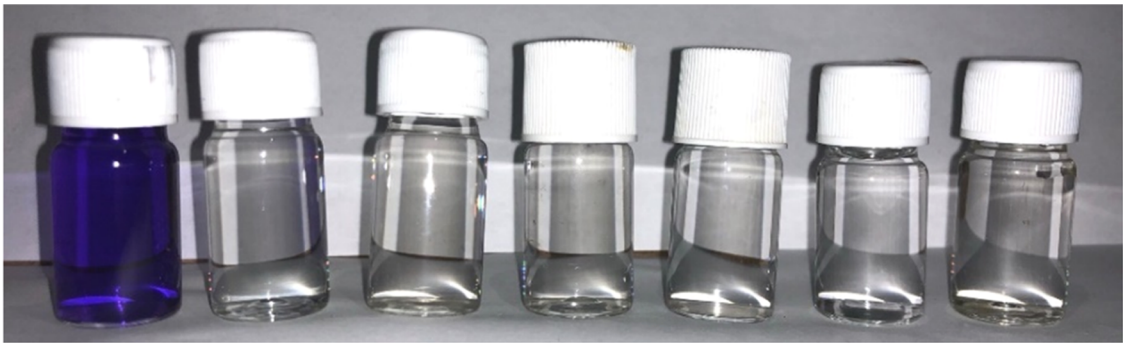

Figure 9. Time-dependent degradation in the flow system.

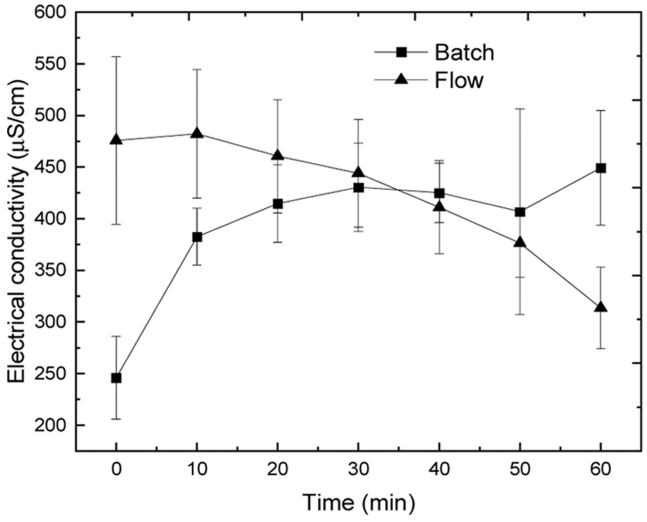

Figure 10. Electrical conductivity in the batch and flow systems.

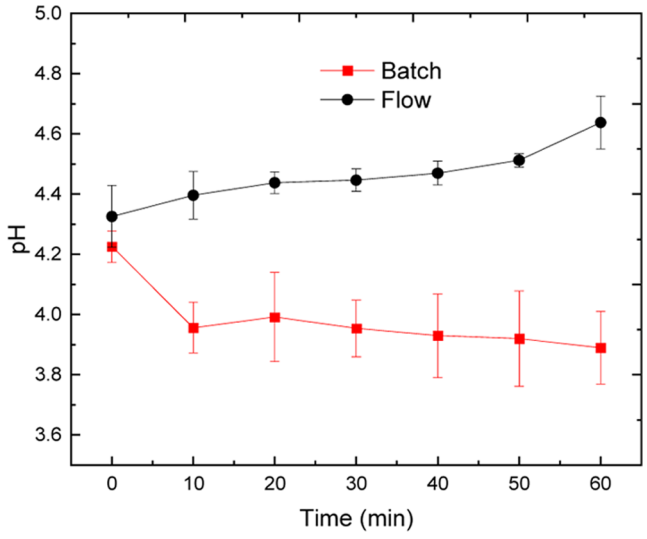

Figure 11. pH in the batch and flow systems.

with the rate constant $k = 2.3 \times 10^{-12} - 1.8 \times 10^{-10}$ cm^3/s (T_e = 1−2 eV).

The recombination of ·OH radicals in the solution produces hydrogen peroxide,[27] as represented in the following reaction (eq 7)

$$\cdot OH + \cdot OH \rightarrow H_2O_2 \text{ rate constant } k = 4 \times 10^{-9} \frac{cm^3}{s} \quad (7)$$

These reactions explain the changes identified in Figures 9 and 10 with respect to the variations in EC and pH.

In addition to the processes established in eqs 6 and 7, iron sulfate provides iron ions (Fe^{2+}), which on reacting with hydrogen peroxide produce OH radicals, as represented in eq 8

$$Fe^{2+} + H_2O_2 \rightarrow Fe^{3+} + OH^- + \cdot OH \quad (8)$$

In acidic solutions, the presence of free protons can influence the formation and stability of nitrites and nitrates, and the interaction between atmospheric plasmas and water in acidic solutions can generate radicals and reactive species that could react with water components to form both nitrites and nitrates. However, in acidic solutions, the relative stability of nitrites is likely to increase compared to nitrates due to their lower tendency to oxidize in an acidic environment.

Dissolved Oxygen and Turbidity. The water oxygenation process is the main characteristic that ensures adequate water quality in the treatment and potabilization processes.[28] Water oxygenation is a process of mass transfer of $O_2 \rightarrow H_2O$, which is largely applied in the following areas: water treatment processes, biological purification of wastewater, separation, and catchment of greases from wastewater.[28]

In the batch-type treatment system, the production of oxygen in the solution is attributed to the generation of bubbles in the anode produced by the dissociation of water: $e^- + H_2O \rightarrow e^- + H + OH$, $e^- + OH \rightarrow e^- + H + O$, and $O + O \rightarrow O_2$.

Figure 12 shows that the value of the measured concentration of dissolved oxygen (DO) in the solution increases gradually as a function of the treatment time for the batch-type system, where the production of bubbles in the anode is to be seen, and consequently an increase in the concentration of DO.

On the other hand, according to Figure 12, the concentration of DO decreases a little and practically remains constant in the solution using the flow treatment system throughout the exposure to plasma. In this case, the production of bubbles is not observed in the anode; and this would explain why there is no increase in the DO concentration. The concentration of DO in the solution affects the production of ·OH radicals and these in turn favor the degradation process of the organic dye.[4]

The change in the turbidity of the treated solution was monitored in the 2 systems, the flow- and the batch-type, every 10 min. Figure 13 shows that in the batch-type system, the

https://doi.org/10.1021/acsomega.3c07559
ACS Omega 2024, 9, 8037−8047

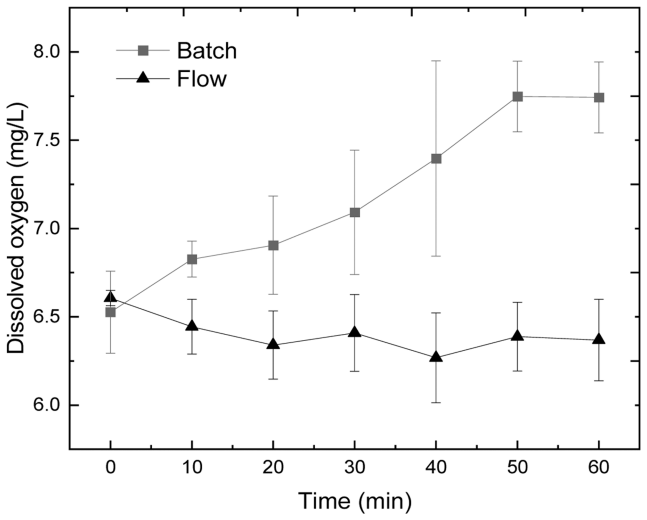

Figure 12. Dissolved oxygen in the batch and flow systems.

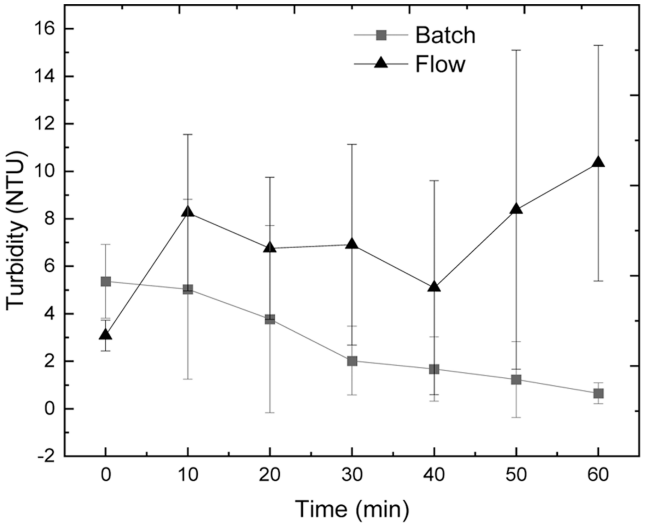

Figure 13. Turbidity in the batch and flow systems.

measured turbidity starts at 5.36 NTU and decreases to a value of 0.65 NTU in 60 min, which represents a decrease of 87.8%. The final solution, as shown in Figure 8, has no suspended particles in sight.

Unlike the turbidity values for the batch-type system, the values in the flow system increase, starting from 3.08 to 10.34 NTU. Physically, Figure 9 shows that the flow-treated solution loses color from the first 10 min, but as floating residues are generated due to the degradation process and the movement of the water, the turbidity values increase.

As a summary, Tables 2 and 3 show the measured values of the monitored parameters of the batch- and flow-type systems, respectively.

Making a qualitative and quantitative comparison based on the color and absorbance of the solution, in the range of time of application of plasma to the samples, it can be inferred that the flow treatment represents a better alternative for the mineralization of this dye.

G_{50}, Electronic Temperature, and Electronic Density. A term constantly used in pollutant degradation processes is the constant known as G_{50},[15,17] which establishes the amount of energy required to degrade 50% of the pollutant in a set volume. Equation 9 establishes the relationship between the constant, initial concentration (C_0), initial volume of the treated sample (V_0), molecular weight of the dye (M), electrical power supplied to the system (P), and the time, in seconds, required to degrade 50% of the contaminant (t_{50}).

$$G_{50} = 1.8 \times 10^6 \frac{C_0 V_0 M}{P t_{50}} \tag{9}$$

In the batch system, an initial concentration of C_0 = 0.01 mM, V_0 = 500 mL, M = 393.96 g/mol, P = 130 W, and t_{50} = 243 s gives a value of $G_{50} = 1.1 \times 10^{-1}$ g/kWh, which indicates that an energy of 1.1×10^{-1} kWh is used to degrade 50% of 1 g of the dye. In the case of the flow system, C_0 = 0.01 mM, V_0 = 5000 mL, M = 393.96 g/mol, P = 300 W, and t_{50} = 189 s gives a value of $G_{50} = 6.3 \times 10^{-1}$ g/kWh. Table 4 shows a comparison of G_{50} values using different degradation methods through atmospheric plasmas and for different dyes.

To describe the electronic temperature and electronic density, considering that the population of the emitting levels follows the Boltzmann distribution and the system has a local thermodynamic equilibrium,[29] the spectral line intensities of H_α and H_β are taken into account for calculating in principle the electronic temperature T_e, according to eq 10

$$T_e = \frac{E_m(2) - E_m(1)}{k} \left[\ln\left(\frac{I_1 \lambda_1 g_m(2) A_m(2)}{I_2 \lambda_2 g_m(1) A_m(1)} \right) \right]^{-1} \tag{10}$$

where $E_m(1)$ denotes the energy of the upper levels of the emission lines, k is the Boltzmann constant, $g_m(1)$ represents the statistical weights of the upper levels, and $A_m(1)$ represents their corresponding transition probabilities. These values were obtained from the NIST atomic spectra database lines.[23,24] In this way, having the value of the electronic temperature, it is possible, using the Saha−Boltzmann equation, to calculate the electronic density using eq 11

$$n_e = 6 \times 10^{21} (T_e)^{3/2} \left(\exp\left[-\frac{E_i}{k T_e} \right] \right) \tag{11}$$

Table 2. Values of the Physical and Chemical Parameters, with Respect to the Interaction Time in a Batch System

Time (min)	pH	Electrical conductivity (μS/cm)	Dissolved oxygen (mg/L)	Turbidity (NTU)	Absorption (a.u.)
0	4.14 ± 0.53	245.90 ± 39.82	6.52 ± 0.23	5.36 ± 1.55	2.59 ± 0.37
10	3.95 ± 0.084	382.50 ± 27.47	6.82 ± 0.10	5.03 ± 3.79	0.37 ± 0.18
20	3.99 ± 0.14	414.50 ± 37.45	6.90 ± 0.27	3.77 ± 3.94	0.07 ± 0.05
30	3.95 ± 0.09	430.40 ± 42.81	7.09 ± 0.35	2.02 ± 1.44	0.05 ± 0.05
40	3.84 ± 0.19	425.00 ± 28.85	7.39 ± 0.55	1.67 ± 1.35	0.09 ± 0.01
50	4.62 ± 1.25	406.80 ± 99.64	7.74 ± 0.2	1.22 ± 1.59	0.03 ± 0.01
60	4.08 ± 0.21	449.20 ± 55.44	7.74 ± 0.2	0.65 ± 0.44	0.04 ± 0.01

https://doi.org/10.1021/acsomega.3c07559
ACS Omega 2024, 9, 8037−8047

Table 3. Values of the Physical and Chemical Parameters, with Respect to the Interaction Time in a Flow System

time (min)	pH	electrical conductivity (μS/cm)	dissolved oxygen (mg/L)	turbidity (NTU)	absorption (a.u.)
0	4.33 ± 0.12	475.8 ± 81.10	6.61 ± 0.04	3.08 ± 0.64	2.61 ± 0.12
10	4.40 ± 0.08	482.2 ± 62.33	6.44 ± 0.15	8.25 ± 3.29	0.15 ± 0.20
20	4.44 ± 0.04	460.6 ± 54.78	6.34 ± 0.19	6.75 ± 2.99	0.06 ± 0.10
30	4.45 ± 0.04	444.0 ± 52.04	6.41 ± 0.21	6.90 ± 4.22	0.03 ± 0.02
40	4.47 ± 0.04	411.0 ± 45.07	6.27 ± 0.25	5.10 ± 4.51	0.02 ± 0.02
50	4.51 ± 0.02	376.4 ± 33.30	6.39 ± 0.19	8.38 ± 6.72	0.03 ± 0.02
60	4.64 ± 0.09	313.6 ± 39.58	6.37 ± 0.23	10.34 ± 4.96	0.03 ± 0.01

Table 4. Values of G_{50} in the Degradation of Dyes through the Application of Different Types of Plasmas

plasma type	pollutant type	sample volume (mL)	power (W)	G_{50} (g/kWh)
corona (batch)	Basic violet I	500	130	0.11
corona (flow)	Basic violet I	5000	300	0.63
DBD	crystal violet	250	5	33.3
DBD	acid red	500	60	
DBD	crystal violet	100	40	
DBD	crystal violet	100	40	
DBD	orange II	500	16.8	3.86
DBD	crystal violet	5	100	0.36
DBD	crystal violet	25		
DBD	crystal violet	100		
DBD	rhodamine B			44.9
corona	indigo carmine	1000	8.6	622
corona	methylene blue			
corona	reactive blue 19	10	1.57	
corona	rhodamine B	1350		11.4
corona	reactive brilliant blue	1000		
corona	methyl orange	450		0.45
corona	Methyl orange	200		
corona	methyl orange	400	5.67	
corona	organic pollutant parachlorophenol	100		
corona	methylene blue	20	4	
corona	methylene blue	100	10	
corona	methyl orange	200		
corona	acid orange 7	600	51	
DBD	methylene blue	300	0.45	
corona	methylene blue	100	0.6	
gliding arc	crystal violet			
gliding arc	reactive blue 137		120	12.7
corona	indigo carmine	500		294
jet	methylene blue	40	150	0.296

where T_e is related to the electronic temperature, E_i represents the ionization energy of the excited species, and k the Boltzmann constant.[30−32]

According to eq 10, the value obtained for electronic temperature T_e is 8.28×10^{-1} eV with an electronic density of 4.15×10^{20}, which was calculated using eq 11. The low electronic temperature is according to a high electronic density due to the higher probability of collision between the electron and ions, having a decrease in the electronic velocities.

CONCLUSIONS

The variables observed in this study indicate a high efficiency in the discoloration of the textile dye Basic Violet I, which is quantified as a function of the interaction time and pH determination, electrical conductivity (μS/cm), dissolved oxygen (mg/L), turbidity (NTU), and absorption spectra (AS). The OES revealed that the presence of the catalyst increased the ·OH production, which favored dye discoloration and reduced the necessary treatment time. A percentage of discoloration of 98.5% of the azo violet I dye was achieved in the maximum process time of 60 min, using plasma and iron sulfate ($FeSO_4$) as the catalyst for the batch system, while for the flow system, at the same time of 60 min, the percentage of discoloration was 98.6%. Both systems were significantly equal in discoloration but at different volumes of 500 and 5000 mL, respectively. The energy yield value (G_{50}) was 1.1×10^{-1} g/kWh for the batch system, while for the flow system, it was 6.3×10^{-1} g/kWh, which implied that the flow system had a lower energy efficiency, although the discoloration time to 50% was less. Through the optical emission spectra of the plasma, different species were identified as ·OH, N_2, H_β, and H_α, identifying the reactions involved in the discoloration process in both systems. The absorption spectra indicate that in the first 10 min of interaction, the process in both systems is effective with a discoloration of 85.7 and 93.9, respectively, with a percentage discoloration of 98.5 and 98.6 at 60 min to the temperature of the solution due to the interaction of the plasma and with the fact that closed and open systems cause a higher or lower interaction of hydrogen ions with the medium. The difference between the values observed in turbidity is due to water movement, which can be quantified from the first 10 min of interaction. Both systems show to be efficient for the discoloration of the Basic Violet I dye, and it is remarkable that it is possible to treat larger volumes of water than those of a batch system with similar results. This makes the implementation of flow systems for the discoloration of water with textile dyes viable on a larger scale, considering that it is a process that requires more electrical energy in the flow system to maintain the discoloration times.

AUTHOR INFORMATION

Corresponding Author

Pedro Guillermo Reyes − *Laboratorio de Física Avanzada, Facultad de Ciencias, Universidad Autónoma del Estado de México, Toluca C.P. 50000, México;* orcid.org/0000-0001-5639-123X; Email: pgrr@uaemex.mx

Authors

Aaron Gomez − *Laboratorio de Física Avanzada, Facultad de Ciencias, Universidad Autónoma del Estado de México, Toluca C.P. 50000, México;* orcid.org/0000-0002-4493-1929

María José Rodríguez Albarrán − *Laboratorio de Física Avanzada, Facultad de Ciencias, Universidad Autónoma del Estado de México, Toluca C.P. 50000, México; Unidad de Irradiación y Seguridad Radiológica, Instituto de Ciencias*

https://doi.org/10.1021/acsomega.3c07559
ACS Omega 2024, 9, 8037−8047

Nucleares, Universidad Nacional Autónoma de México, Ciudad de México C.P. 04510, México; orcid.org/0000-0001-7857-2621

Josefina Vergara Sanchez − *Facultad de Ciencias Químicas e Ingeniería, Universidad Autónoma del Estado de Morelos, Cuernavaca C.P. 62209 Morelos, México;* orcid.org/0000-0003-2001-7208

Cesar Torres − *Laboratorio de Análisis y Sustentabilidad Ambiental, Escuela de Estudios Superiores de Xalostoc, Universidad Autónoma del Estado de Morelos, Ayala C.P. 62715, México;* orcid.org/0000-0002-1125-3148

Daniel Osorio − *Laboratorio de Biofísica Molecular, Facultad de Ciencias, Universidad Autónoma del Estado de México, Toluca C.P. 50000, México*

Horacio Martínez − *Laboratorio de Espectroscopia, Instituto de Ciencias Físicas, Universidad Nacional Autónoma de México, Cuernavaca C.P. 62210, México*

Hugo Saldarriaga − *Centro de Investigaciones Químicas, Instituto de Investigación en Ciencias Básicas y Aplicadas, Universidad Autónoma del Estado de Morelos, Cuernavaca C.P. 62209 Morelos, México*

Complete contact information is available at: https://pubs.acs.org/10.1021/acsomega.3c07559

Notes

The authors declare no competing financial interest.
[○]PhD student.

■ ACKNOWLEDGMENTS

The authors thank the projects DGAPA [IN102222], CONACyT [268644], UAEMex 6743/2022CIB, and PRODEP [CA-5511-6/18-8304] and C. Amado for their technical assistance.

■ GLOSSARY

BVI, Basic Violet I; OES, optical emission spectra; G_{50}, energy yield; AOPs, advanced oxidation processes; MV, methyl violet; $FeSO_4$, iron sulfate; EC, electrical conductivity; NTU, nephelometric turbidity unit; NIST, atomic spectra database lines; AS, absorption spectra

■ REFERENCES

(1) Wang, S.; Ruan, Y.; Sun, H.; Yi, L.; Liu, D.; Wang, J.; Zhang, Z.; Fang, D. Study on degradation of Basic Violet 1 and heat generation by parallel orifice plate hydrodynamic cavitation. *Process Saf. Environ. Prot.* **2022**, *168*, 285−299, DOI: 10.1016/j.psep.2022.09.063. ISSN

(2) Salazar, R.; Garcia-Segura, S.; Ureta-Zañartu, M.; Brillas, E. Degradation of Disperse Azo Dyes from Water by Solar Photoelectro-Fenton. *Electrochim. Acta* **2011**, *56*, 6371−6379.

(3) Khataee, A.; Gholami, P.; Vahid, B. Heterogeneous sono-Fenton-like process using nanostructured pyrite prepared by Ar glow discharge plasma for treatment of a textile dye. *Ultrason. Sonochem.* **2016**, *29*, 213 DOI: 10.1016/j.ultsonch.2015.09.012.

(4) Lee, H.; Park, S. H.; Cheong, C.-J.; Kim, S.-J.; Seo, S.-G.; Park, Y.-K.; Jung, S.-C. Contribution of Dissolved Oxygen to Methyl Orange Decomposition by Liquid Phase Plasma Processes System. *Ozone: Sci. Eng.* **2014**, *36* (3), 244−248, DOI: 10.1080/01919512.2013.874277.

(5) Allabakshi, S. M.; Srikar, P.; Gangwar, R. K.; Maliyekkal, S. M. Treatment of azo, direct, and reactive dyes in surface dielectric barrier discharge: Valorization of effluent, the influence of wastewater characteristics, and plasma modeling by Stark broadening technique. *J. Water Process Eng.* **2023**, *56*, No. 104503, DOI: 10.1016/j.jwpe.2023.104503.

(6) Vergara, J.; Torres, C.; Montiel, E.; Gómez, A.; Reyes, P. G.; Martínez, H. Degradation of textile dye AB 52 in an aqueous solution by applying a plasma at atmospheric pressure. *IEEE Trans. Plasma Sci.* **2017**, *45*, 479−484, DOI: 10.1109/TPS.2017.2663845.

(7) Ali, I.; Kon'kova, T.; Liberman, E.; Simakina, E.; ALOthman, Z. A.; Alomar, T. S.; Islame, M. A. Preparation and characterization of SnO_2-CeO_2 nanocomposites: Sorption, modeling and kinetics for azorubine dye removal in water. *J. Mol. Liq.* **2022**, *346* (15), No. 117119, DOI: 10.1016/j.molliq.2021.117119.

(8) Moyo, S.; Makhanya, B. P.; Zwane, P. E. Use of bacterial isolates in the treatment of textile dye wastewater: A review. *Heliyon* **2022**, *8*, No. e09632.

(9) Barrera, H.; Cruz-Olivares, J.; Frontana-Uribe, B. A.; Gómez Díaz, A.; Reyes-Romero, P. G.; Barrera-Díaz, C. E. Electro-Oxidation-Plasma Treatment for Azo Dye Carmoisine (Acid Red 14) in an Aqueous Solution. *Materials* **2020**, *13* (6), No. 1463, DOI: 10.3390/ma13061463.

(10) Jinzhang, G. G.; Xiao, M.; Dongping, Y. W. The Role of Fe (II) in the Contact Glow Discharge Electrolysis. *Plasma Sci. Technol.* **2007**, *9*, No. 431, DOI: 10.1088/1009-0630/9/4/10.

(11) Moradi, H.; Kim, D.-S.; Yang, J.-K.; Chang, Y.-Y.; Park, S.-B.; Kamranifard, T. Synergy of cold plasma and sulfate radicals in the treatment of dye-contaminated wastewater; mechanistic study of the degradation mechanism using DFT. *Sep. Purif. Technol.* **2023**, *323*, No. 124381, DOI: 10.1016/j.seppur.2023.124381.

(12) Dihom, H. R.; Al-Shaibani, M. M.; Mohamed, R. M. S. R.; Al-Gheethi, A. A.; Sharma, A.; Khamidun, M. H. B. Photocatalytic degradation of disperse azo dyes in textile wastewater using green zinc oxide nanoparticles synthesized in plant extract: A critical review. *J. Water Process Eng.* **2022**, *47*, No. 102705, DOI: 10.1016/j.jwpe.2022.102705.

(13) Wang, X.; Zhou, M.; Jin, X. Application of glow discharge plasma for wastewater treatment. *Electrochim* **2012**, *83*, 501−512 Acta.

(14) Locke, B. R.; Thagard, S. M. Analysis and review of chemical reactions and transport processes in pulsed electrical discharge plasma formed directly in liquid water. *Plasma Chem. Plasma Process* **2012**, *32* (5), 875 DOI: 10.1007/s11090-012-9403-y.

(15) Malik, M. A.; Ghaffar, A.; Malik, S. A. Water purification by electrical discharges. *Plasma Sources Sci. Technol.* **2001**, *10* (1), 82 DOI: 10.1088/0963-0252/10/1/311.

(16) Malik, M. A. Water Purification by Plasmas: Which Reactors are Most Energy Efficient? *Plasma Chem. Plasma Process.* **2010**, *30*, 21−31.

(17) Rahimpour, M.; Taghvaei, H.; Zafarnak, S.; Rahimpour, M. R.; Raeissi, S. Post-discharge DBD plasma treatment for degradation of organic dye in water: A comparison with different plasma operation methods. *J. Environ. Chem. Eng.* **2019**, *7* (4), No. 103220, DOI: 10.1016/j.jece.2019.103220.

(18) Hameed, B. H. Equilibrium and kinetic studies of methyl violet sorption by agricultural waste. *J. Hazard. Mater.* **2008**, *154* (1−3), 204 DOI: 10.1016/j.jhazmat.2007.10.010.

(19) Diamante, C.; Bergfeld, W. F.; Belsito, D. V.; Klaassen, C. D.; Marks, J. G., Jr; Shank, R. C.; Slaga, T. J.; Snyder, P. W.; Alan Andersen, F. Final report on the safety assessment of Basic Violet 1, Basic Violet 3, and Basic Violet 4. *Int. J. Toxicol.* **2009**, *28* (6 Suppl2), 193S−204S. PMID: 20086192

(20) Hamza, M.; Abdelhedi, R.; Brillas, E.; Sirés, I. Comparative electrochemical degradation of the triphenylmethane dye Methyl Violet with boron-doped diamond and Pt anodes. *J. Electroanal. Chem.* **2009**, *627*, 41−50, DOI: 10.1016/J.JELECHEM.2008.12.017.

(21) Anzai, K.; Aoki, T.; Koshimizu, S.; Takaya, R.; Tsuchida, K.; Takajo, T. Formation of reactive oxygen species by the irradiation of cold atmospheric pressure plasma to water. *Free Radical Biol. Med.* **2018**, *120*, S64.

(22) Girard, F.; Badets, V.; Blanc, S.; Gazeli, K.; Marlin, L.; Authier, L.; Svarnas, P.; Sojic, N.; Clément, F.; Arbault, S. Formation of reactive nitrogen species including peroxynitrite in physiological

buffer exposed to cold atmospheric plasma. *RSC Adv.* **2016**, *6* (82), 78457 DOI: 10.1039/C6RA12791F.
(23) NIST https://www.nist.gov/.
(24) Pearse, R. W. B.; Gaydon, A. G. *The Identification of Molecular Spectra*; Chapman and Hall Ltd: London, 1976.
(25) Jiang, B.; Zheng, J.; Qiu, S.; Wu, M.; Zhang, Q.; Yan, Z.; Xue, Q. Review on electrical discharge plasma technology for wastewater remediation. *Chem. Eng. J.* **2014**, *236*, 348−368.
(26) Ghodbane, H.; Hamdaoui, O.; Vandamme, J.; Durme, J. V.; Vanraes, P.; Leys, C.; Nikiforov, A. Y. Degradation of AB25 dye in liquid medium by atmospheric pressure non-thermal plasma and plasma combination with photocatalyst TiO_2. *Open Chem.* **2015**, *13*, 325−331, DOI: 10.1515/chem-2015-0040.
(27) Sarangapani, Ch.; Misra, N. N.; Milosavljevic, V.; Bourke, P.; O'Regan, F.; Cullen, P. J. Pesticide degradation in water using atmospheric air cold plasma. *J. Water Process Eng.* **2016**, *9*, 225−232, DOI: 10.1016/J.JWPE.2016.01.003.
(28) Mihaela, C. I.; Nicolae, B.; Adrian, C. The Determination of Dissolved Oxygen Concentration in Stationary Water. *Appl. Mech. Mater.* **2013**, *436*, 233−237.
(29) Raju, G. G. Collision cross sections in gaseous electronics part I: what do they mean? *IEEE Electr. Insul. Mag.* **2006**, *22*, 5−23.
(30) Unnikrishnan, V. K.; Alti, K.; Kartha, V. B.; Santhosh, C.; Gupta, G. P.; Suri, B. M. Measurements of plasma temperature and electron density in laser-induced copper plasma by time-resolved spectroscopy of neutral atom and ion emissions. *Pramana* **2010**, *74*, 983−993.
(31) Griem, H. R. *Principles of Plasma Spectroscopy*; Cambridge University Press: United Kingdom, 1997.
(32) Feng, J.; Wang, Z.; Li, Z.; Ni, W. Study to reduce laser-induced breakdown spectroscopy measurement uncertainty using plasma characteristic parameters. *Spectrochim. Acta, Part B* **2010**, *65*, 549−556.

https://doi.org/10.1021/acsomega.3c07559
ACS Omega 2024, 9, 8037−8047